Quadrupole and Octupole Excitations of the Even Tin Isotopes by Electron Scattering*

T. H. CURTIS,† R. A. EISENSTEIN,‡ D. W. MADSEN, AND C. K. BOCKELMAN
Yale University, New Haven, Connecticut 06520
(Received 16 December 1968)

Form factors obtained by the inelastic scattering of 60-MeV electrons from the first 2^+ and 3^- collective states of Sn^{116}, Sn^{118}, and Sn^{120} are reported. The momentum transfer range covered is 0.3–0.6 F^{-1}. Reduced transition probabilities $B(EL)$ and transition radii R_{tr}^2 are extracted from the data, using a transition charge distribution with a radial dependence given by the derivative of a Fermi charge distribution, and the distorted-wave code DUELS. In addition, the parameters c and t for a ground-state Fermi charge distribution, obtained by elastic scattering, are reported for Sn^{116}, Sn^{118}, Sn^{120}, and Sn^{124}.

I. INTRODUCTION

THE continuing improvement of microscopic theories of nuclear collective motion justifies the considerable experimental effort directed to refining the accuracy with which the revelant parameters are known. In these theories the electromagnetic matrix elements describing transitions between collective states play a central role, since prediction of experimental results from the model wave functions is straightforward. Most of the available data are derived from radioactive decay, Coulomb excitation, and resonance fluorescence experiments; accuracies of the order of 10% in the reduced radiative transition probability $B(E2)$ linking the ground state to the first quadrupole excited state are typical, and improvement to the order of 5% has been achieved in favorable cases. The lowest octupole state generally lies at a higher excitation than the lowest quadrupole state; the lower accuracies of $B(E3)$ reflect the greater experimental problems involved. However, reduced radiative transition probabilities do not afford complete tests of the electromagnetic aspects of nuclear models, since they measure only the Lth radial moment of the transition charge and current densities. To define these transition densities more completely, inelastic electron scattering experiments are particularly valuable since they furnish the greater momentum transfer necessary to measure higher radial moments without sacrificing the essential simplicity of a purely electromagnetic interaction.

The present results for certain of the even isotopes of tin are presented in the hope they may contribute useful input to the understanding of nuclear structure. Relevant microscopic calculations of collective properties of the Sn nuclei have been published by Arvieu *et al.*[1] and by Sawicki and collaborators[2–4]; more detailed calculations are underway. For certain of the lowest 2^+ and 3^- states, experimental results of electron scattering in the momentum transfer range 0.6–0.9 F^{-1} have been published by Barreau and Bellicard.[5] The present experiments cover the range 0.3–0.6 F^{-1}, nicely connecting the Coulomb excitation work to the higher-energy electron scattering.

The absolute cross sections necessary for interpretation of the results are obtained by comparison with elastic scattering measurements. Although the systematics developed by Elton[6] from Stanford measurements permit reasonable prediction of the elastic electron scattering from Sn, recent measurements at Stanford on the Ca isotopes[7] have reemphasized the importance of possible isotopic variations in the ground-state charge density. At the time the present work was initiated, no such data had been published for the Sn nuclei. Therefore elastic scattering measurements were also undertaken and are here reported.

II. EXPERIMENTAL ARRANGEMENT

The experiment was performed with conventional equipment. A beam of several microamperes average current at energies up to 60 MeV analyzed to $\pm 0.2\%$ in energy is available from the Yale Electron Accelerator. The beam was incident on foils of metallic tin, nominally $1\times1\times0.001$ in., enriched to greater than 95% isotopic purity in Sn^{116}, Sn^{118}, Sn^{120}, and Sn^{124}. To ensure target uniformity and stability under bombardment, the targets were placed $\frac{1}{4}$ in. off center and were rotated[8] at 1 revolution/sec. Polyethylene foils approximately 0.030 in. thick were used as hydrogen targets for elastic scattering cross-section normalization. In addition, the beam was defocused to a 2×2-mm square, and kept below 0.6 mA. Since energy resolution was not a serious problem in the present experiment, the use of this large a beam spot pre-

* Supported in part by the Atomic Energy Commission, under Contract No. (30-1)2726, with Yale University.
† Present address: Experimental Physics, Lawrence Radiation Laboratory, Livermore, Calif.
‡ Present address: Weizmann Institute, Department of Nuclear Physics, Rehovoth, Israel.
[1] R. Arvieu, E. Baranger, M. Baranger, M. Veneroni, and V. Gillet, Phys. Letters **4**, 119 (1963).
[2] P. L. Ottaviani, M. Savoia, and J. Sawicki, Phys. Letters **24B**, 353 (1967).
[3] M. Gmitro and J. Sawicki, Phys. Letters **26B**, 493 (1968).
[4] A. Rimini, J. Sawicki, and T. Weber, Phys. Rev. **168**, 1401 (1968).
[5] P. Barreau and J. B. Bellicard, Phys. Rev. Letters **19**, 1444 (1967).
[6] L. R. B. Elton, *Nuclear Sizes* (Oxford University Press, New York, 1961).
[7] R. Hofstadter, G. K. Noldeke, K. J. van Oostrum, L. R. Suelzle, M. R. Yearian, B. C. Clark, R. Herman, and D. G. Ravenhall, Phys. Rev. Letters **15**, 758 (1965); K. J. van Oostrum, R. Hofstadter, G. K. Noldeke, M. R. Yearian, B. C. Clark, R. Herman, and D. G. Ravenhall, *ibid.* **16**, 528 (1966); R. F. Frosch *et al.*, Phys. Rev. **174**, 1380 (1968).
[8] The target rotators were designed and constructed by G. A. Peterson and E. A. Comeau.

TABLE I. Summary of corrections to elastic scattering data.

	Correction	A Magnitude of correction (%)	B Uncertainty of correction (%)	$A\times B$ Uncertainty introduced (%)	Quantity affected by correction or uncertainty
(a)	Counting losses	<2	10	0.2	Data point
(b)	Dispersion	0–15	0.05	0.008	Data point
(c)	Background	<1	20	0.2	Data point
(d)	Radiative correction				
	ΔS	<20	5	1	Peak area
	ΔB	<5	5	0.25	Peak area
(e)	Landau correction	...	...	...	Peak area
(f)	Isotopic purity	5	2	0.1	c, t
(g)	Multiple scattering	...	...	...	Peak area
(h)	Statistics			~3/pt	Data point
(i)	Target thickness			3	Cross section
(j)	Scattering angle	<0.5	5	0.025	Cross section
(k)	Incident energy			0.2	Cross section
(l)	Accuracy of computer program			0.1	c, t

sented no difficulty. The elastic scattering from each target was checked before and after each run; the peaks reproduced to within counting statistics in height (better than 0.1%), and to better than $\frac{1}{6}$ of the peak width in position. The excellent reproducibility ensured that neither target deterioration nor significant energy shift had occurred during the run.

The targets were placed on the axis of a scattering chamber, about which rotated a 16-in. radius $n=\frac{1}{2}$ magnetic spectrometer. Electrons were detected in a set of plastic scintillator counter telescopes in the spectrometer focal surface. The over-all energy resolution was 0.3% or better. Normalization of different runs was obtained by integration of the beam current transmitted to a Faraday cup. Further details of the experimental arrangement are as given earlier,[9] except for replacement of the current integrator by a Model 1000, manufactured by the Rogers Instrument Co., Brookhaven, N.Y.

[9] M. A. Duguay, C. K. Bockelman, T. H. Curtis, and R. A. Eisenstein, Phys. Rev. **163**, 1259 (1967).

Data handling was greatly facilitated by use of an on-line PDP-8 computer interfaced to scalers which registered the electron pulses. Under computer control the scalers were reset to zero, started, and the digital output of the current integrator counted. When the required amount of charge was collected, the scalers were stopped, and their contents were simultaneously typed out from storage and punched on paper tape. At the end of each run, the contents of the memory were transferred to magnetic tape via an off-line PDP-7 computer. Corrections to the data and theoretical calculations described below were performed using the 7090-7094 Direct-Coupled-System at the Yale Computer Center.

III. ELASTIC SCATTERING

A. Procedure

The elastic cross sections for tin were determined by comparing them to the known electron-proton scattering cross section. First, a tin elastic peak was taken

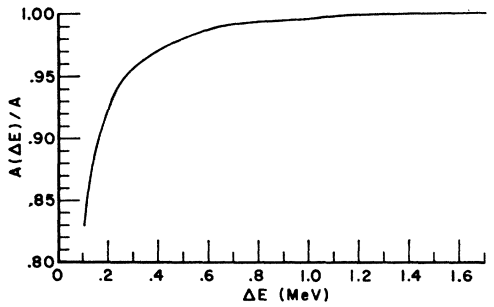

FIG. 1. Approach of corrected elastic-peak area $A(\Delta E)$ to constant value A as the cutoff ΔE increases.

in 25-keV steps, from slightly above the elastic peak to about 1 MeV below, extending out on the radiative tail. Counting times were increased on the tail to improve statistics. Then a proton elastic peak was obtained by scattering from CH_2. These data were corrected for spectrometer dispersion, dead-time losses, and background as explained in Sec. III B. Because the hydrogen peak is superimposed on the radiative tail from the carbon peak, points were taken from approximately 1 MeV above to 1 MeV below the proton peak. The radiative tail of the carbon peak was fitted, using the points of the high-energy side of the proton peak, with a curve of the form

$$Y=A/\Delta E+B/(\Delta E)^2.$$

Here ΔE is the separation in gauss between a point on the background curve and the position of the carbon elastic peak, and A and B are determined by least-squares fitting. This shape for the radiative tail has been used successfully at Darmstadt[10] and Yale.[11,12] This curve was then extrapolated under the proton peak and subtracted to obtain the area of the hydrogen peak.

B. Corrections and Errors

A number of corrections had to be applied to the raw data and peak areas, and to the energies and angles used to calculate the theoretical cross section. These corrections are summarized in Table I, and explained more fully below:

(*a*) *Counting losses.* The dead-time loss circuit used has been described in Ref. 11. The accuracy of the correction was determined from experimental tests.

(*b*) *Dispersion.* Each of the detectors takes a constant percentage energy "bite" out of the spectrum of scattered electrons. The width in energy of this "bite" decreases as lower electron energies are measured. To correct for this decrease the well-known dispersion correction must be applied:

$$\text{true counts}\sim(\text{observed counts})\times 1/\text{field},$$

where "field" is the value of the magnetic field of the spectrometer for the detected electron.

(*c*) *Background.* This was determined by looking at the high-energy side of the elastic peak, where no counts are expected, and assuming a constant background. The main source of background appears to be neutrons produced when the electron beam is stopped in the Faraday cup.

(*d*) *Radiative corrections.* When an electron scatters from the nucleus it will emit a bremsstrahlung γ ray due to its change in velocity. If the γ ray has sufficiently high energy, the scattered electron will not be detected as part of the elastic peak. No matter how far out in the elastic-peak radiative tail a cutoff is applied, there is still a finite probability that some "elastically" scattered electrons will have lost enough energy by radiation to miss being counted. The correction factors are given by[13–15]

$$\Delta S=(2\alpha/\pi)\{[\tfrac{1}{2}\ln(E_0/\eta^2\Delta E)+\tfrac{1}{2}\ln(E_0/\eta\Delta E)-13/12]$$
$$\times[2\ln(q/mc^2)-1]+17/36+\tfrac{1}{2}[\tfrac{1}{6}\pi^2-L_2(\cos^2(\tfrac{1}{2}\theta))]\}$$

and

$$\Delta B=(t/x\ln 2)[\tfrac{1}{2}\ln(E_0/\eta^2\Delta E)+\tfrac{1}{2}\ln(E_0/\eta\Delta E)],$$

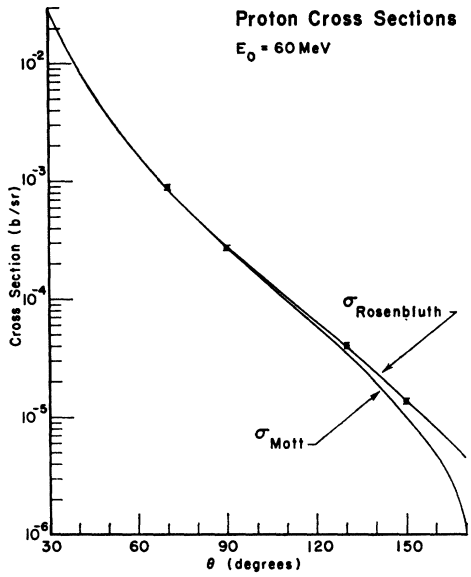

FIG. 2. Mott and Rosenbluth cross sections for scattering of electrons from a proton, with experimental points. The data were arbitrarily normalized to make the 90° point fit the curve. $E_0=60$ MeV.

[10] F. Gudden and P. Strehl, Z. Physik **185**, 111 (1965); E. Spamer, *ibid.* **191**, 24 (1966); H. Liesem, *ibid.* **196**, 174 (1966); O Titze and F. Spamer, Z. Naturforsch. **21a**, 1504 (1966); M. Stroetzel and F. Gudden, Phys. Letters **22**, 485 (1966); E. Spamer and H. Artus, Z. Physik **198**, 445 (1967).

[11] M. A. Duguay, thesis, Yale University, 1966 (unpublished).

[12] J. F. Ziegler, thesis, Yale University, 1967 (unpublished); J. F. Ziegler and G. A. Peterson, Phys. Rev. **165**, 1337 (1968).

[13] H. Bruer, University of Saskatchewan Report No. SAL-4 (unpublished).

[14] H. Crannell, Phys. Rev. **148**, 1107 (1966).

[15] J. W. Motz, H. Olsen, and H. W. Koch, Rev. Mod. Phys. **36**, 881 (1964).

where α is the fine-structure constant 1/137.04,

$$q=(2E_0/\hbar c)\sin(\tfrac{1}{2}\theta)[1+2E_0\sin^2(\tfrac{1}{2}\theta)/Mc^2]^{-1/2},$$

E_0 is the incident electron energy, mc^2 is the rest mass of electron (=0.511 MeV), η is the recoil factor [$=1+2E_0\sin^2(\frac{1}{2}\theta)/Mc^2$], Mc^2 is the rest mass of target, θ is the scattering angle, ΔE is the cutoff point on radiative tail, t is the target thickness as seen by incident electron (see below), and x is the radiation length for the target material.

$$L_2(a)=-\int_0^a \frac{\ln(1-u)}{u}\,du$$

is the Euler dilogarithm. By expanding $\ln(1-u)$, dividing by u, and integrating term by term, the approximation

$$L_2(a)=a+\tfrac{1}{4}a^2+\tfrac{1}{9}a^3+\cdots=\sum_{n=1}^{\infty}(a^n/n^2)$$

can be made. Ten terms give this to four-place accuracy for $a=0$–1, which is the region of interest for this calculation.

The correction is applied using the formula

$$(d\sigma/d\sigma)_{\text{expt}}=(d\sigma/d\Omega)_{\text{obs}}\times\exp[\delta(\Delta E)],$$

where $\delta(\Delta E)=\Delta S+\Delta B$. The value of the corrected area should be independent of the cutoff ΔE. The approach to a constant value is shown in Fig. 1. As can be seen, for $\Delta E\geq 0.8$ MeV the area is reasonably constant. The same cutoff point $\Delta E=0.9$ MeV was chosen for all data to reduce systematic error.

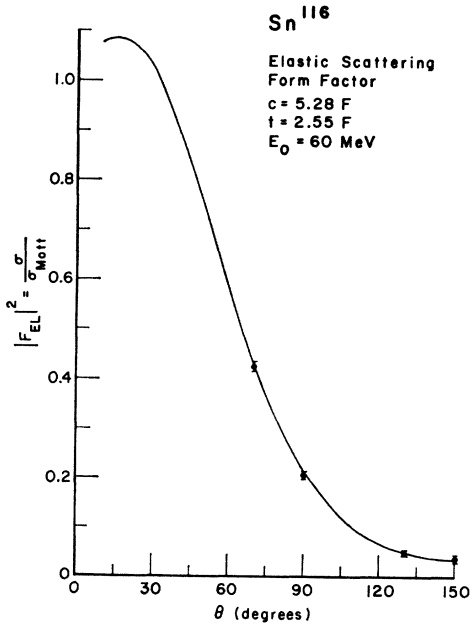

FIG. 3. Best fit of elastic scattering data for Sn^{116}, obtained with $c=5.28$ F, $t=2.55$ F.

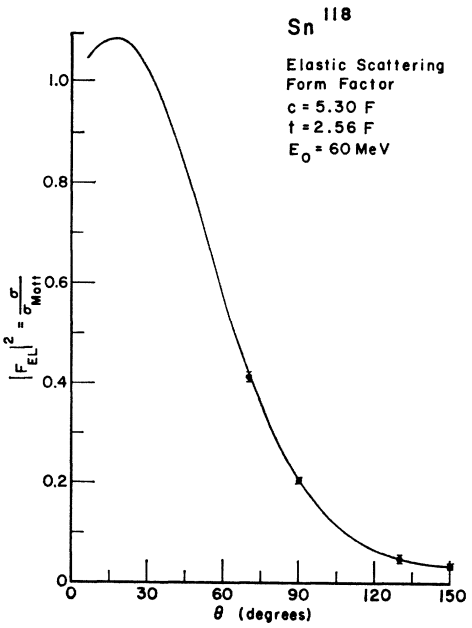

FIG. 4. Best fit of elastic scattering data for Sn^{118}, obtained with $c=5.30$ F, $t=2.56$ F.

(*e*) *Landau correction.* The straggling (uncertainty) of the electron energy loss in passing through the target makes it possible that an electron would lose enough energy to elastically scatter and not be detected. However, the energy loss is ~50 keV, so straggling was on the order of ~15 keV. For a $\Delta E=0.9$ MeV, the Landau correction factor[16] is negligible.

(*f*) *Isotopic purity.* The isotopes (prepared in the form of metal foils by the Oak Ridge National Laboratory) had the following enrichments: Sn^{116}, 95.6%; Sn^{118}, 97.1%; Sn^{120}, 98.4%; and Sn^{124}, 94.7%. In each case impurities other than tin were negligible. Hence, scattering from other isotopes contributes at most 5% to the cross sections. Since the parameters of the ground-state charge distribution for each tin isotope differ by no more than 2%, the error introduced in the ground-state parameters is of the order of $5\times 2\%=0.1\%$.

(*g*) *Multiple scattering.* At the very highest counting rate observed for elastic scattering, less than 1 out of 10^4 electrons is scattered. Thus, the probability of multiple scattering is an appropriate power of this (10^{-4}, 10^{-8}) and is vanishingly small.

(*h*) *Statistics.* Each datum point was weighted by $N^{-1/2}$ in determining least-squares fits and adding up peak areas.

(*i*) *Target thickness.* This was the greatest source of uncertainty in determining the absolute values of the cross sections. Two methods were used to determine the thickness: (1) weighing the target and measuring the

[16] L. Landau, J. Phys. (USSR) **8**, 201 (1944).

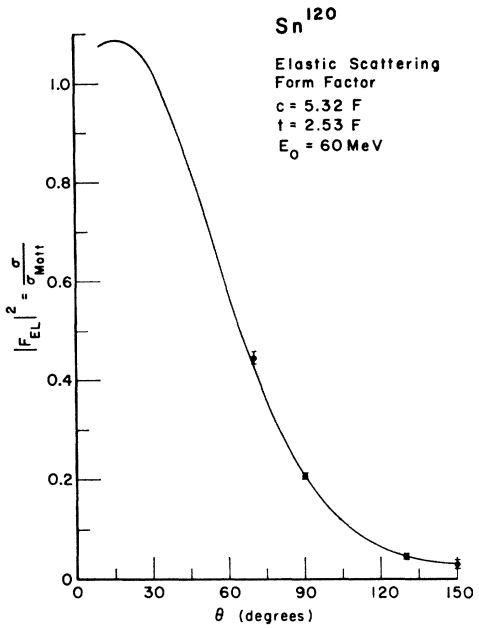

FIG. 5. Best fit of elastic scattering data for Sn^{120}, obtained with $c=5.32$ F, $t=2.53$ F.

area with a planimeter and (2) measuring the thickness with a micrometer and using the known density. The two methods gave identical results within the limits of error. Both of these methods assume a uniform target thickness; since the targets were rotated in the beam, any nonradial nonuniformities in target thickness were averaged over.

(*j*) *Scattering angle.* Three important corrections had to be applied to the nominal scattering angle:

(1) The entrance port of the spectrometer is at a azimuthal angle $\beta=54'$ with respect to the plane in which the scattering angle is measured. Hence the correction $\cos\theta=\cos\theta'\cos\beta$ had to be applied.

(2) A correction is necessary because the spectrometer subtends a finite angular range in the scattering plane. The cross section changes rapidly with scattering angle; this change makes the mean scattering angle (weighted by cross section) different from the median scattering angle (central ray of the collimator). The correction to the scattering angle is $\Delta=\frac{1}{2}\epsilon\alpha$, where α is the rate of change in the cross section over an angular interval ϵ. The value of α (6% per degree at 90°) was calculated for both H and Sn by assuming an angular dependence which varied as the Mott cross section. ϵ had the value 1°12′.

(3) The lab–center-of-mass transform is essentially unity for the Sn nucleus. For the scattering from hydrogen, the inclusion of the recoil term in the Rosenbluth formula (below) takes into account the lab–c.m. transformation. The nominal scattering angles θ' were determined by calibrating a divided circle centered on the target and bolted to the floor.

(*k*) *Incident energy.* The energy E' of the scattered electron was determined from the spectrometer calibration.[17] To determine the incident energy E_0 of the electrons we used the formula $E_0=E'+E_R+\frac{1}{2}E_L$, where E' is the energy of the scattered electron, E_R is the recoil energy of the nucleus, and E_L is the calculated energy loss of the electron passing through the target.

C. Experimental Results

After correcting the data, the areas under the peaks were determined by summing the counts. The total number of counts under an elastic peak is given by

$$N=\sigma\rho Q\Omega, \quad (1)$$

where N is the number of counts under peak after corrections, σ is the differential cross section, ρ is the number of nuclei per unit area, Q is the number of incident particles, and Ω is the "effective solid angle," a term which contains the geometric solid angle and other terms not measured individually but assumed to remain constant while scattering from Sn or CH_2. They are (1) efficiency of detector, (2) efficiency of beam collection, and (3) calibration of beam integrator.

The proton cross section was calculated using the Rosenbluth formula[18]

$$\sigma_p(\theta)=\sigma_{\text{Mott}}\{1+(q^2/4M^2)\times[2(1+\mu)^2\tan^2(\tfrac{1}{2}\theta)+\mu^2]\}, \quad (2)$$

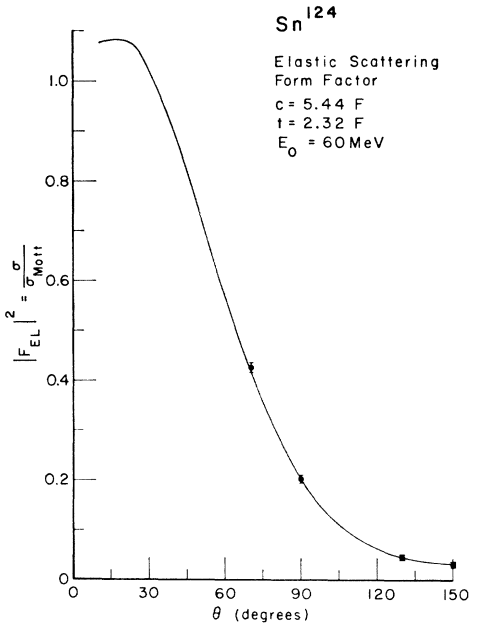

FIG. 6. Best fit of elastic scattering data for Sn^{124}, obtained with $c=5.44$ F, $t=2.32$ F.

[17] R. A. Eisenstein, Yale University Electron Accelerator Internal Report (unpublished).

[18] M. N. Rosenbluth, Phys. Rev. 79, 615 (1950).

TABLE II. Summary of elastic scattering data.

Isotope	E_0 (MeV)	θ	Peak area (arb. units) Sn	H	σ_p (b/sr)	Ω (arb. units)	σ_{Sn}^{expt} (b/sr)	σ_{Sn}^{calc} (b/sr)
116	60.137	70.00	1.095×10^3	0.970	0.8557×10^{-3}	1.13×10^3	0.951±3%	0.9618
116	60.137	89.95	1.68×10^2	0.315	0.2740×10^{-3}	1.15×10^3	0.147±3%	0.1531
116	60.181	129.75	5.48	0.0448	0.3860×10^{-4}	1.16×10^3	0.480×10^{-2}±3%	0.4837×10^{-2}
116	60.174	149.64	1.19	0.0148	0.1386×10^{-4}	1.07×10^3	0.1039×10^{-2}±4%	0.9753×10^{-3}
118	59.932	70.00	1.10×10^3	0.970	0.8617×10^{-3}	1.13×10^3	0.938±3%	0.9675
118	60.041	89.95	1.69×10^2	0.314	0.2749×10^{-3}	1.14×10^3	0.149±3%	0.1522
118	59.976	129.75	5.50	0.0443	0.3885×10^{-4}	1.15×10^3	0.482×10^{-2}±2½%	0.4858
118	60.038	149.64	1.14	0.0162	0.1391×10^{-4}	1.16×10^3	0.100×10^{-2}±3%	0.9706×10^{-3}
120	60.137	70.00	1.085×10^3	0.970	0.8557×10^{-3}	1.13×10^3	1.00±2½%	0.9513
120	60.137	89.95	1.71×10^2	0.315	0.2740×10^{-3}	1.15×10^3	0.149±2½%	0.1502
120	60.181	129.75	5.35	0.0448	0.3860×10^{-4}	1.16×10^3	0.447×10^{-2}±2½%	0.4690×10^{-2}
120	60.174	149.64	1.085	0.0148	0.1386×10^{-4}	1.07×10^3	0.102×10^{-2}±3%	0.9512×10^{-3}
124	59.932	70.00	1.09×10^3	0.970	0.8617×10^{-3}	1.13×10^3	0.973±3%	0.9557
124	60.041	89.95	1.69×10^2	0.314	0.2749×10^{-3}	1.14×10^3	0.146±4%	0.1483
124	59.976	129.75	5.30	0.0443	0.3885×10^{-4}	1.15×10^3	0.463×10^{-2}±4%	0.4649×10^{-2}
124	60.038	149.64	1.085	0.0162	0.1391×10^{-4}	1.16×10^3	0.963×10^{-3}±4%	0.9523×10^{-3}
						average: 1.14×10^3		

where

$$\sigma_{\text{Mott}} = (e^4/4E_0^2)[\cos^2(\tfrac{1}{2}\theta)/\sin^4(\tfrac{1}{2}\theta)] \times[1+(2E_0/Mc^2)\sin^2(\tfrac{1}{2}\theta)]^{-1},$$

$$\mu = 1.79\,\mu_N.$$

This formula predicts the elastic scattering of electrons from a point charge with a magnetic moment. The cross sections σ_p and σ_{Mott} are plotted in Fig. 2. The experimental proton cross-section values are also plotted, with the 90° point arbitrarily normalized to fit the curve. The data clearly show the magnetic-moment contribution. The proton charge form factor was taken to be 1 which is accurate to better than 1.0% in this energy region.[19]

The calculated proton cross section was used with the experimental data to determine Ω for each run. The data are listed in Table II. In particular, column 7 lists the effective solid angles; their constancy is a measure of the over-all reproducibility of the experiment, and their variation is consistent with the final error assigned. The average value of Ω, together with the corrected ratios of the Sn- to H-peak areas, was used to obtain the values of the Sn cross sections listed in column 8 of Table II and graphed in Figs. 3–6.

TABLE III. Comparison of elastic scattering results.

Isotope	This work c (F)	t (F)	$\langle r^2\rangle^{1/2}$ (F)	χ^2 of fit	Barreau and Bellicard[a] c (F)	t (F)
Sn^{116}	5.28±0.03	2.55±0.025	4.62	1.07	5.275±0.025	2.37±0.05
Sn^{118}	5.30±0.03	2.56±0.025	4.64	0.71		
Sn^{120}	5.32	2.53	4.64	2.44	5.315±0.025	2.53±0.05
Sn^{124}	5.44±0.03	2.32±0.025	4.64	0.77	5.440±0.030	2.37±0.05

[a] Reference 22.

[19] R. Hofstadter, F. Bumiller, and M. R. Yearian, Rev. Mod. Phys. **30**, 482 (1958).

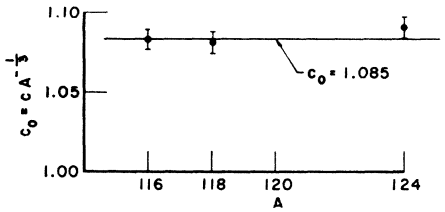

FIG. 7. $A^{1/3}$ dependence of $c_0 = cA^{-1/3}$. The straight line is the best least-squares fit to the three points.

In order to compute the errors on the cross sections, the errors summarized in Table I were all treated as random. All errors which contribute to the uncertainty of individual data points were compounded by taking the square root of the sum of the squares of the individual errors. These uncertainties were used in determining least-squares fits to the radiative tail and in calculating the error in peak areas. The errors in peak area were compounded with the other errors in Table I (again using the square root of the sum of the squares) to give the final errors quoted in Table II.

D. Analysis of Data

For the analysis of the elastic scattering, a Fermi charge distribution has been assumed:

$$\rho(r) = \rho_0\{1+\exp[(r-c)/a]\}^{-1}, \qquad (3)$$

where the half-density radius c is the point at which $\rho(r) = \frac{1}{2}\rho_0$ and $t = 4.4a$ is the skin thickness or distance over which $\rho(r)$ changes from $0.9\rho_0$ to $0.1\rho_0$. The numerical phase-shift code of Rawitscher and Fischer[20] was used to calculate elastic cross sections for given c and t; these calculations were fitted to the experimental data. Figures 3–6 display the best fits.

The best-fit parameters c and t are determined by calculating the elastic scattering cross sections for many sets of c and t and comparing them with the experimental cross section. The best-fit values are taken as those which minimize the quantity

$$\chi^2 = \frac{1}{n}\sum_{i=1}^{N}\frac{(\sigma_{i,\text{theoret}}-\sigma_{i,\text{expt}})^2}{(\Delta\sigma_{i,\text{expt}})^2}, \qquad (4)$$

where $\sigma_{i,\text{theoret}}$ is the ith theoretical cross section, $\sigma_{i,\text{expt}}$ is the ith experimental cross section, $\Delta\sigma_{i,\text{expt}}$ is the error of ith experimental cross section, N is the number of data points, and n is the degrees of freedom ($N-2$ in this case). The errors used in this calculation are essentially the cross-section errors of Table II. These errors dominate the slight uncertainties introduced by computational error in the Rawitscher-Fischer program and by the target impurities.

The results of these fits and their χ^2 values are given in Table III. The errors assigned the best-fit values of c and t are determined from the range of values of c and t which yield a χ^2 less than the 68% confidence level value of χ^2. For two degrees of freedom, this confidence level corresponds to a (normalized) $\chi^2 < 1.2$. For the Sn^{120} case the minimum value of χ^2 obtained was 2.4; a value of χ^2 this large would appear randomly with less than 10% probability. This is taken to indicate that at least one of the data points had a significant undetected systematic error. Because of this it is not possible to assign an error for the Sn^{120} parameters.

An alternative and instructive way of viewing elastic scattering results was pointed out by Feshbach, who showed analytically that for low-momentum transfer scattering ($q < 0.4$ F^{-1}) one may expect to extract only one model-independent parameter: the mean-square radius $\langle r^2\rangle$ of the ground-state charge distribution. Further, Engfer[21] has demonstrated, using the Darmstadt elastic scattering code, that the cross section for 60-MeV scattering by Ti is indeed determined by $\langle r^2\rangle$. For a Fermi distribution, the mean-square radius is related to c and t by

$$\langle r^2\rangle = \tfrac{3}{5}[c^2+(7/3)\pi^2a^2], \qquad a/c \ll 1. \qquad (5)$$

The rms radii computed from the best-fit c and t are also listed in Table III. For the present results it is noted that, although the *minimum* χ squares are obtained for the c, t values cited in Table III, low values of χ square are also obtained for the family of pairs of c, t which satisfy Eq. (5) for the $\langle r^2\rangle$ computed from the best-fit c and t. However, extreme values of c and t are excluded.

E. Comparison with Other Results

Recently Barreau and Bellicard[22] have reported results of 150-MeV elastic electron scattering on Sn^{116}, Sn^{120}, and Sn^{124}, and have extracted the values of c and t listed in Table III. The present results agree with those of Barreau and Bellicard,[22] except for the value of t for Sn^{116}.

In order to see whether the measured radii indicate deviation from an $A^{1/3}$ law, the values of c have been fitted, using a least-squares criterion, to the equation $c = c_0A^{1/3}$. Excluding the value for Sn^{120} because of its indeterminate error, the present work leads to a value of $c_0 = 1.085 \pm 0.005$. In Fig. 7, the three values of c, divided by $A^{1/3}$, are plotted against A together with the straight line $c_0 = 1.085$. The error bars assigned to the individual values of R just overlap the straight line; thus there is no significant deviation observed from an $A^{1/3}$ dependence, in apparent contradiction to the claim of Barreau and Bellicard.[22]

Values for differences in $\langle r^2\rangle$ are available from measurements of optical and muonic x-ray isotope shifts. The present data do not disagree with existing

[20] G. H. Rawitscher and C. R. Fischer, Phys. Rev. 122, 1330 (1961); C. R. Fischer and G. H. Rawitscher, *ibid.* 135, B377 (1964).

[21] R. Engfer, Z. Physik 192, 29 (1966).

[22] P. Barreau and J. B. Bellicard, Phys. Letters 25B, 470 (1967).

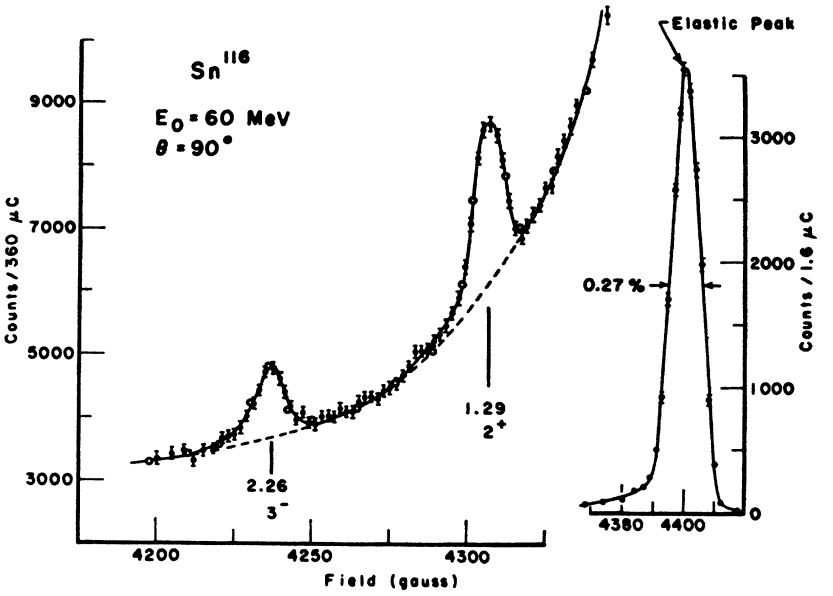

FIG. 8. Typical spectrum of scattered electrons, from Sn^{116}, $E_0=60$ MeV, 90° scattering angle. The data points have had no corrections applied.

measurements for the isotopes of Sn,[23–25] but do not measure this difference with sufficient accuracy to allow significant comparison.

IV. INELASTIC SCATTERING

A. Data Reduction

The techniques used in obtaining and reducing the inelastic scattering data have been discussed in an earlier publication.[9] Briefly, the experimental quantity desired is the square of the inelastic form factor $|F_{in}|^2$ as a function of the momentum transfer q_I for each of the nuclear levels excited. Recalling the definition of a form factor,

$$|F_{in}|^2=\sigma_{in}/\sigma_{Mott}=(\sigma_{in}/\sigma_{el})\sigma_{el}/\sigma_{Mott}=R|F_{el}|^2, \quad (6)$$

where σ_{in} is the scattering cross section to an excited level, σ_{el} is the elastic scattering cross section, and σ_{Mott} is the Mott scattering cross section [see Eq. (2)].

The ratio R of inelastic to elastic cross sections was obtained by comparing the areas of the inelastic and elastic scattering peaks, properly normalized for spectrometer dispersion and charge collection. The best values of c and t obtained from the elastic scattering measurements were used to calculate the elastic cross section with the Rawitscher-Fischer phase-shift program[20] and hence $|F_{el}|^2$ was calculated.

It may appear that a needless extra step has been inserted, namely, the extraction of c and t from the elastic scattering data and then the recalculation of $|F_{el}|^2$ using these c and t. However, c and t may be regarded as merely a convenient parameterization of σ_{el} which relieves the necessity of having to make a careful measurement of σ_{el} and σ_p for each datum point. Noting only the incident energy and scattering angle at which R was measured, and computing $|F_{el}|^2$ for the exact incident energy and scattering angle, a precise determination of $|F_{in}|^2$ was made using Eq. (6). Typically from run to run over a period of weeks, the incident energy might be set at energies differing by about 200–300 keV.

A typical spectrum of scattered electrons is shown in Fig. 8. These are the observed data with no corrections applied. The elastic peak has a typical resolution of 0.27% and a radiative tail which extends from the low-energy side. The inelastic levels, taken in this case with 225 times the charge, appear as peaks riding on the tail of the elastic peak. The excellent reproducibility of the system is indicated by the open points on the inelastic spectrum, which were points retaken at the completion of the spectrum.

The data were first corrected for dead-time losses, dispersion, and background as explained in Sec. III. The shape of the inelastic peak was taken to be the same as the shape of the elastic peak, but multiplied by a constant factor, which is correct only if the radiative corrections for the elastic peak and the inelastic peak are the same. These corrections were calculated, using the formula of Sec. III B (d), and for low excitation energies (<3.5 MeV) they were found to be the same to better than 0.5%. The constant multiplying factor is then just the ratio R of inelastic to elastic scattering. The inelastic peaks are superimposed on the radiative tail of the elastic peak. Recalling the discussion of

[23] S. Devons, T. T. Bardin, R. C. Barrett, R. C. Cohen, D. Hitlin, E. Macagno, C. Nissim-Sabat, J. Rainwater, K. Runge, and C. S. Wu, Phys. Rev. Letters **16**, 718 (1966).
[24] R. D. Ehrlich, D. Fryberger, D. A. Jensen, C. Nissim-Sabat, R. J. Powers, V. L. Telegdi, and C. K. Hargrove, Phys. Rev. Letters **18**, 959 (1967); R. Ehrlich, Phys. Rev. **173**, 1088 (1968).
[25] W. H. King, H. G. Kuhn, and D. N. Stacey, Proc. Roy. Soc. (London) **A296**, 24 (1967); D. N. Stacey, Proc. Roy. Soc. (London) **A280**, 439 (1964).

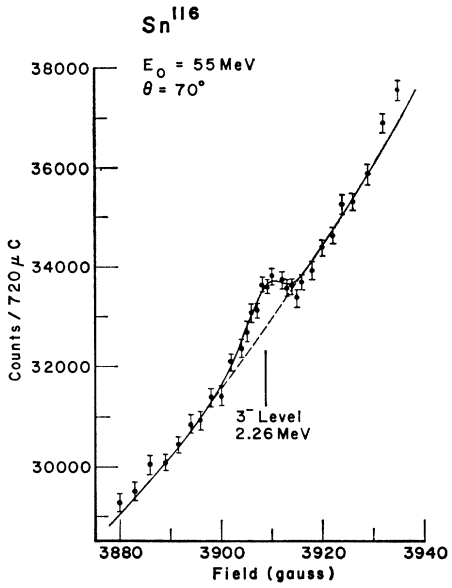

FIG. 9. Fit of the elastic-peak shape to the inelastic data for the 3^- level at 2.26 MeV in Sn^{116}.

Sec. III A, the inelastic spectra were fitted using an equation of the form

$$Y_i = \frac{A}{\Delta E} + \frac{B}{(\Delta E)^2} + \sum_{j=1}^{N} R_j \times (\text{elastic-peak shape}),$$

where N is the number of peaks. The coefficients A, B, and R_j were determined using a least-squares fitting routine.

The program also varied the position of the inelastic peak over a small range to obtain the best fit. This enabled accurate determinations of the excitation energies. Typical fits of this program to the data are shown in Figs. 9–11.

The results of this least-squares fitting procedure for each of the data points taken is shown in Table IV, which lists E_0, θ', q_I, $|F_{el}|^2$, R, $|F_{in}|^2$, statistical error, and χ^2 for each level studied.

B. Levels Observed

The isotopes Sn^{116}, Sn^{118}, and Sn^{120} were each studied up to 4 MeV in excitation, with the specific purpose of observing the collective 2^+ and 3^- levels. The scattering angles were 70°, 90°, 110°, 130°, and 150° at 60-MeV and 70° at 55-MeV incident energy. This corresponds to a momentum transfer (q_I) range of 0.31–0.58 F^{-1}. In addition, Sn^{116} was further explored to 12 MeV in excitation at 150°, 60 MeV. No other excitations comparable in strength were observed.

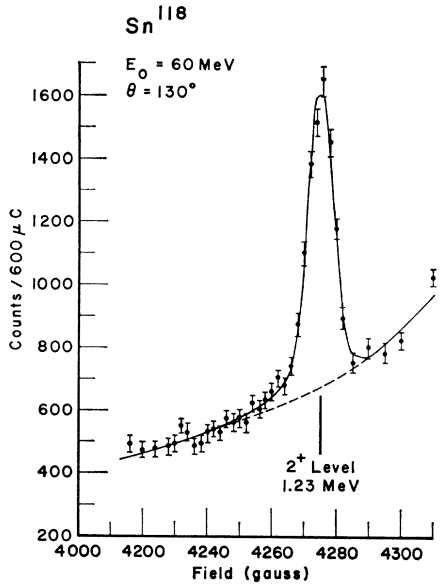

FIG. 10. Fit of the elastic-peak shape to the inelastic data for the 2^+ level at 1.23 MeV in Sn^{118}.

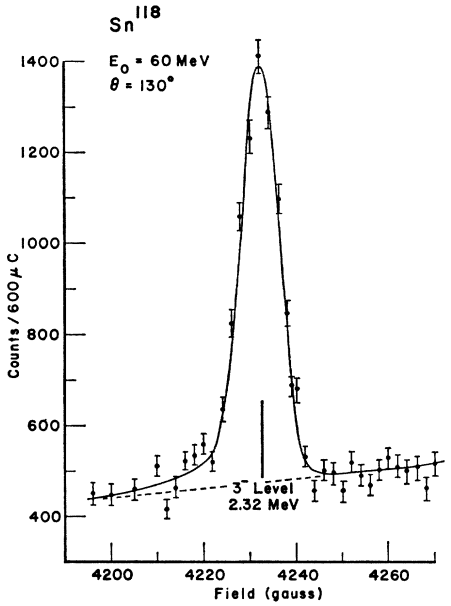

FIG. 11. Fit of the elastic-peak shape to the inelastic data for the 3^- level at 2.32 MeV in Sn^{118}.

Figure 12 shows the known energy levels for Sn^{116}, Sn^{118}, and Sn^{120} below 4 MeV, as observed in inelastic proton scattering.[26] The transitions measured in the present experiment are indicated by arrows. Considering the experimental resolution, it is evident that several states may contribute to the peaks associated with the 3^- levels. Although small contribution from nearby levels cannot be excluded, the peak shapes and angular distributions in each case are consistent with pure $E3$ excitation.

[26] D. L. Allan, B. H. Armitage, and B. A. Doran, Nucl. Phys. **66**, 481 (1965).

TABLE IV. Summary of inelastic scattering data.

E_0 (MeV)	θ (deg)	q_I (F^{-1})	$\lvert F_{el}\rvert^2$	10^4R	$10^4\lvert F_{in}\rvert^2$	Error (%)	χ^2
			Sn^{116}				
			2^+ level at 1.29 MeV				
55.15	70	0.317	0.532	6.52	3.37[a]	10	2
60.11	70	0.346	0.435	8.41	3.66	15	2
60.17	90	0.426	0.213	31.83	6.77	6	1.5
60.13	90	0.426	0.213	31.08	6.63	5	1.2
60.68	110	0.498	0.093	93.05	8.65	2	1.2
60.64	110	0.498	0.051	85.01	7.94	4	1.3
60.12	130	0.546	0.051	146.36	7.39	2	1.3
60.15	130	0.546	0.050	153.39	7.72	2	1.4
59.49	150	0.576	0.037	184.94	6.83	5	0.6
			3^- level at 2.26 MeV				
55.16	70	0.314	0.532	0.91	0.47[a]	20	1.5
60.12	70	0.343	0.434	1.13	0.49	20	4.0
60.14	90	0.423	0.213	12.75	2.72	8	1.6
60.65	110	0.494	0.093	46.60	4.34	3	1.8
60.68	110	0.494	0.093	47.26	4.39	3	1.6
60.14	130	0.542	0.050	119.75	6.04	3	1.5
60.18	130	0.542	0.050	129.98	6.53	3	1.6
59.44	150	0.571	0.037	196.95	7.31	4	1.6
			Sn^{118}				
			2^+ level at 1.23 MeV				
55.16	70	0.317	0.528	6.65	3.41[a]	20	4
60.10	70	0.346	0.431	9.91	4.27	8	1.6
60.17	90	0.427	0.209	34.59	7.24	3	2.1
60.13	90	0.426	0.210	32.04	6.73	4	1.8
60.15	110	0.494	0.096	77.50	7.42	4	1.7
60.21	110	0.495	0.095	81.70	7.78	2	1.5
60.17	130	0.547	0.049	150.37	7.37	2	1.2
60.20	130	0.547	0.049	166.12	8.11	4	1.2
59.43	150	0.576	0.036	177.95	6.46	3	1.0
			3^- level at 2.32 MeV				
55.18	70	0.314	0.527	1.42	0.73[a]	20	2.4
60.11	70	0.343	0.430	1.80	0.77	15	1.9
60.14	90	0.423	0.210	10.37	2.18	9	2.0
60.17	90	0.423	0.209	13.97	2.92	4	1.1
60.17	110	0.490	0.096	43.45	4.15	5	1.7
60.21	110	0.490	0.095	48.30	4.60	2	1.2
60.18	130	0.542	0.049	124.69	6.10	3	0.8
60.18	130	0.542	0.049	121.53	5.94	3	1.2
59.45	150	0.570	0.036	199.18	7.22	3	1.3

TABLE IV. (*Continued*).

E_0 (MeV)	θ' (deg)	q_I (F^{-1})	$\lvert F_{EL}\rvert^2$	10^4R	$10^4\lvert F_{in}\rvert^2$	Error (%)	χ^2
			Sn^{120}				
			2^+ level at 1.16 MeV				
54.98	70	0.316	0.530	6.42	3.31[a]	15	2
60.12	70	0.346	0.429	10.31	4.42	8	2
60.18	90	0.427	0.208	30.79	6.42	4	1.5
60.13	90	0.427	0.209	30.29	6.33	5	1.9
60.21	110	0.495	0.095	87.53	8.28	3	1.5
60.15	110	0.494	0.095	79.70	7.58	4	1.5
60.21	130	0.548	0.048	151.74	7.34	3	1.6
60.21	130	0.548	0.048	151.71	7.34	3	1.8
59.53	150	0.577	0.036	169.89	6.07	4	1.4
			3^- level at 2.39 MeV				
54.99	70	0.313	0.530	1.15	0.59[a]	20	1.8
60.12	70	0.342	0.429	1.60	0.69	30	1.8
60.15	90	0.422	0.209	10.51	2.19	10	2.8
60.18	90	0.423	0.208	12.68	2.64	4	1.5
60.18	110	0.489	0.095	38.51	3.65	6	1.7
60.21	110	0.490	0.095	44.76	4.23	3	1.3
60.18	130	0.542	0.049	115.71	5.62	4	1.5
60.21	130	0.542	0.048	116.75	5.65	3	1.3
59.54	150	0.571	0.036	185.62	6.63	4	1.6

[a] Data normalized from 55 to 60 MeV (see text).

C. Distorted-Wave Analysis

The angular distributions of the inelastically scattered electrons were analyzed using the code DUELS of Tuan *et al.*[27] In using this code it is necessary to assume, in addition to the ground-state charge distribution, transition charge and current densities. For the ground-state charge distributions the parameters cited in Table III were used; for the transition charge density the form assumed was

$$\rho_{tr}(r)=N_L r^{L-1}(d/dr)\{1+\exp[(r-c_{tr})/a_{tr}]\}^{-1},$$
$$a_{tr}=t_{tr}/4.4. \quad (7)$$

Following Ref. 27, the quantities "radius variation" (V_R) and "skin variation" (V_S) are defined by

$$V_R=c_{tr}/c \quad \text{and} \quad V_S=t_{tr}/t,$$

where c and t describe the ground-state charge distribution. Thus $V_R=V_S=1$ implies a pure hydrodynamic or "Tassie" model.[28] The code includes the contributions of the current distribution implied by the continuity equation. The calculated curves are normalized to $B(EL\uparrow)=1\ e^2\ F^{2L}$; thus the factor by which the theoretical curves must be multiplied to fit the data is the $B(EL\uparrow)$ for the transition.

The fits of the calculated form factors to the data

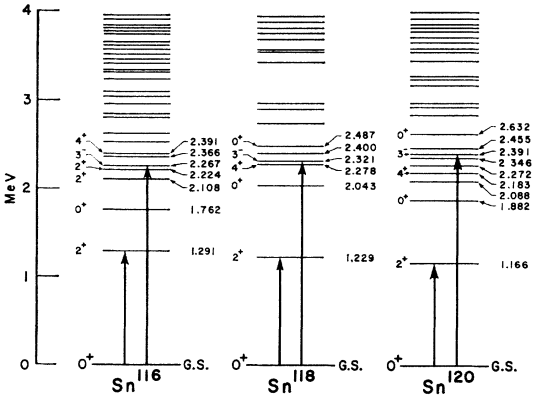

FIG. 12. Energy levels of Sn^{116}, Sn^{118}, and Sn^{120} according to Allan *et al.* (Ref. 26). The levels studied in the present experiment are indicated by arrows.

[27] S. T. Tuan, L. E. Wright, and D. S. Onley, Nucl. Instr. Methods **60**, 70 (1968), and references therein.
[28] L. J. Tassie, Nuovo Cimento **5**, 1497 (1957).

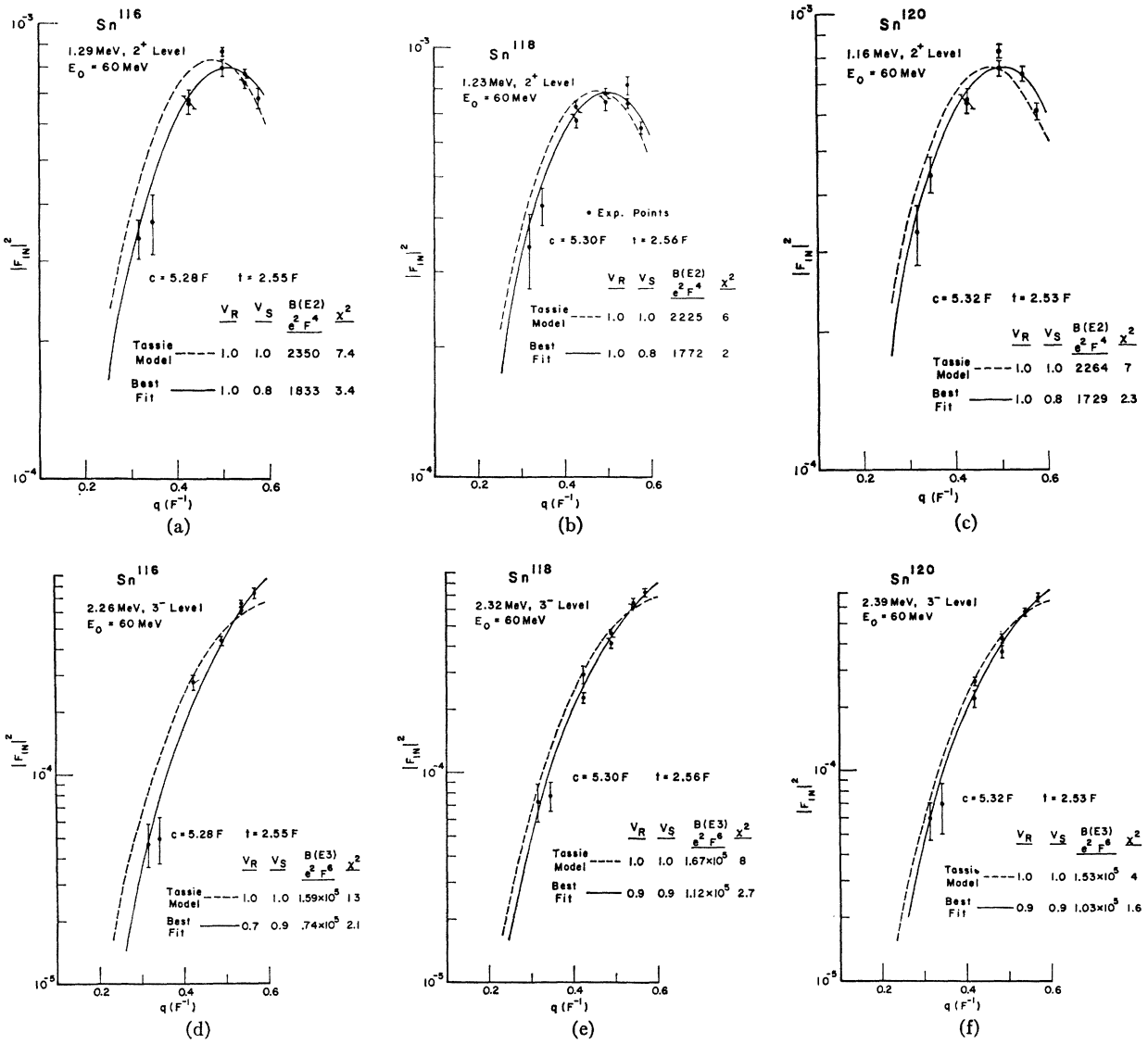

FIG. 13. Fit of code DUELS form-factor curves to data points. The Tassie model cannot reproduce the shape of the experimental points.

TABLE V. Summary of inelastic scattering results.

Isotope	E_x (MeV)	Tassie model $B(EL\uparrow)$ (e^2F^{2L})	V_R	V_S	Best fit $B(EL\uparrow)$ (e^2F^{2L})	R_{tr}^2 (F^2)	χ^2
Sn^{116}	1.29 2^+	2350	1.0	0.8	1833	35.9	3.4
Sn^{118}	1.23 2^+	2225	1.0	0.8	1722	35.9	1.9
Sn^{120}	1.16 2^+	2264	1.0	0.8	1729	35.9	2.3
Sn^{116}	2.26 3^-	1.59×10^5	0.7	0.9	0.74×10^5	30.0	2.1
Sn^{118}	2.32 3^-	1.67×10^5	0.9	0.9	1.12×10^5	37.8	2.7
Sn^{120}	2.39 3^-	1.53×10^5	0.9	0.9	1.03×10^5	37.8	1.6

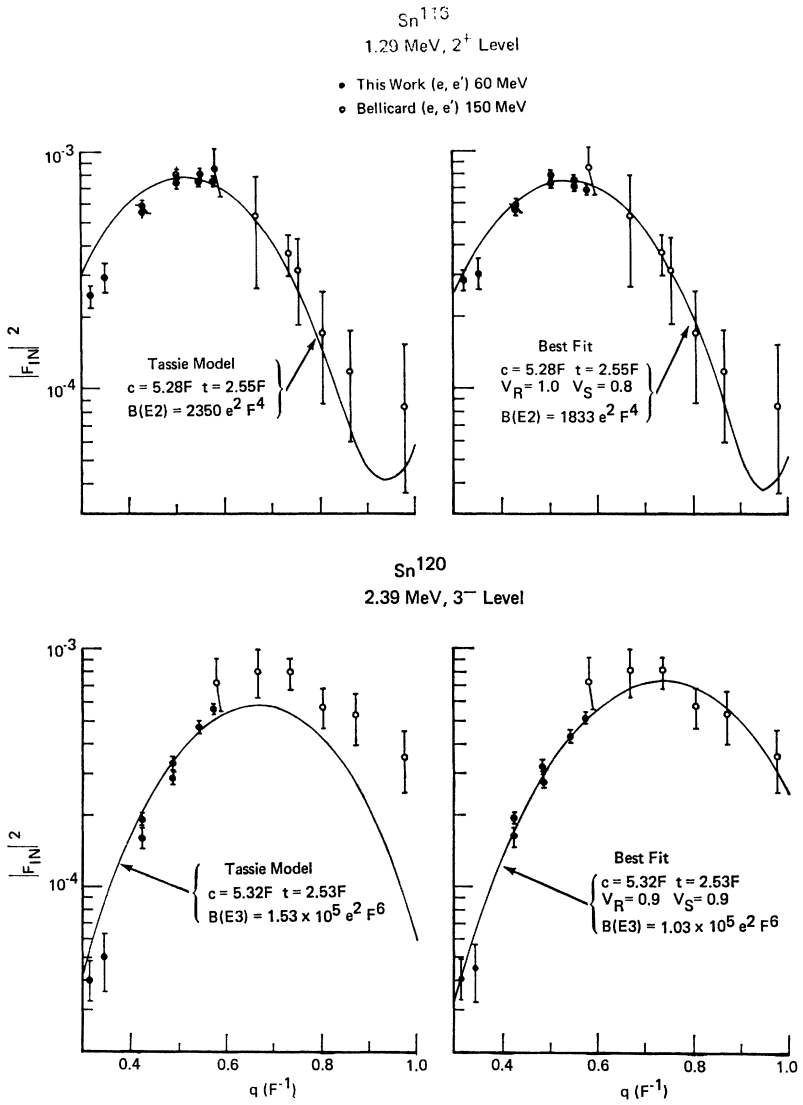

FIG. 14. Comparison of this work to that of Barreau and Bellicard (Ref. 5).

are shown in Fig. 13. The dashed line shows the Tassie model predictions. The solid line gives the best fit to the data, obtained by varying V_R and V_S. The results are summarized in Table V. For the 2^+ levels, the values $V_R=1.0$ and $V_S=0.8$ are found to provide the best fits to each of the three sets of data. This corresponds to a ρ_{tr} which is peaked at the surface of the nucleus, but is narrower than the surface vibration (Tassie) model predicts. For the 3^- levels the values $V_R=0.9$ and $V_S=0.9$ provide the best fits for the excitations of Sn^{118} and Sn^{120}. The 3^- level in Sn^{116} requires $V_R=0.7$ and $V_S=0.9$.

A further indication of the transition charge deviations may be obtained by comparing the present results with those of Barreau and Bellicard.[5] These authors measured the inelastic scattering of 150-MeV electrons from the lowest 2^+ and 3^- states in Sn^{116}, Sn^{120}, and Sn^{124}; their momentum transfer range ($q=0.6$–1.0 F^{-1}) complements the present data. The data for the 2^+ level in Sn^{116} and the 3^- level in Sn^{120} shown in Fig. 14 are typical. To make comparison the 60-MeV data were normalized to the 150-MeV data using code DUELS for both the Tassie model and the best-fit values of V_R and V_S. Figure 14 indicates that the two experiments are in excellent agreement, provided that the best-fit parameters are used.

Table V also lists values of the square of the transition radius R_{tr} obtained from the best-fit values of ρ_{tr}. This quantity, the ratio of the $L+2$ radial moment to the Lth radial moment of ρ_{tr}, is discussed in Ref. 9.

D. Comparison with Other Results

An obvious difficulty in making exact comparison of the $B(EL)$ from different experiments is the lack of

TABLE VI. Comparison of results for $B(EL\uparrow)$ (single-particle units).

Isotope	E_x (MeV)	J^π	Single-particle unit (e^2 F^{2L})	This work	(e, e')[a]	(α, α')[b]	(α, α')[c] ±20%	Coulomb excitation ±20%	(d, d') ±40%	Resonance fluorescence ±20%
Sn^{116}	1.29	2^+	167	10.5	12	24	17	12[d]		20[e]
Sn^{118}	1.23	2^+	172	11		19	10	14[d]		17[f]
Sn^{120}	1.16	2^+	175	10	10	14	15	13[d]	15[g]	9[f]
Sn^{122}	1.14	2^+	180			14	17	15[d]		
Sn^{124}	1.13	2^+	184		10	10		12[d]		
Sn^{116}	2.26	3^-	5.64×10^3	14.9	34	22	23	38[h]	57[i]	
Sn^{118}	2.32	3^-	5.90×10^3	18.5		16	23	28[h]	28[i]	
Sn^{120}	2.39	3^-	6.05×10^3	17.5	30	12	20	22[h]	20[g]	
Sn^{122}	2.42	3^-	6.26×10^3			11	20	34[h]		
Sn^{124}	2.61	3^-	6.45×10^3		18	5		22[h]		

[a] Reference 5.
[b] Reference 33.
[c] Reference 32.
[d] Reference 36.
[e] Reference 38.
[f] Reference 39.
[g] Reference 34.
[h] Reference 37.
[i] Reference 35.

meaningful error assignments in many cases, including the present data. If our error analysis (which follows the outline sketched in Sec. III B) were correct, the χ^2 values listed in Table V indicate that even the best fit is unsatisfactory. The 95% confidence level for χ^2 for 6 or 7 degrees of freedom is 2; there is only a 5% chance that the best fits could be the proper ones and yet have χ^2 exceed this value. Four out of the six cases studied have $\chi^2>2$. For this reason it has not been possible to assign conventional errors to the reduced radiation transition probabilities reported herein. Quantitive assignment of errors awaits a model which fits the data, as well as a more sophisticated error treatment than here attempted. Still the comparisons cited below have qualitative significance.

The reduced transition probabilities to the levels studied in this experiment have been measured previously using a variety of experimental techniques, including (e, e') at 150 MeV, (α, α'), (d, d'), Coulomb excitation, and resonance fluorescence. The results of these experiments are tabulated in Table VI and compared with the values obtained in this experiment. The $B(EL)$'s have been expressed as multiples of the single-particle unit (SPU), defined by

$$B(EL)_{\mathrm{SPU}}=[(2L+1)/4\pi]\{[3/(3+L)]eR^L\}^2,$$

where $R=1.2A^{1/3}$.

e,e' Experiment

The discussions of the previous section have indicated that the present data are consistent with the measurements of Barreau and Bellicard.[5] However, the value of $B(E3)$ quoted in Ref. 5 is distinctly larger than given in Table V. We surmise that the difference may lie in the use of the Born approximation in deriving the values of Ref. 5.

(α, α') and (d, d') Experiments

The analysis of inelastic α-particle scattering (and other heavy-charged-particle scattering) may be carried out using either a Blair-Fraunhofer[29] optical diffraction model or a distorted-wave Born approximation (DWBA), as described in Ref. 30. The result of either of these analyses is a number β_L, the nuclear deformation parameter. If the nuclear charge and mass distributions have the same shape, the $B(EL\uparrow)$ from the ground state ($R=R_0$) to the excited state is related to β_L by

$$B(EL\uparrow)=[(3/4\pi)ZeR_0^L]^2\beta_L^2. \quad (8)$$

It is necessary[31] to multiply the β_L obtained from the heavy-particle scattering (which we shall call β_{HP}) by the ratio R_{HP}/R_0, where R_{HP} is the strong-absorption radius of the optical analysis and R_0 is the charge-distribution radius used to obtain

$$\beta_{EM}=\beta_{\mathrm{HP}}(R_{\mathrm{HP}}/R_0)$$

before using Eq. (8). This is because β_{HP} does not measure directly the charge-distribution deformation, but contains additional contributions from the finite

[29] J. S. Blair, Phys. Rev. **115**, 928 (1959).
[30] R. H. Bassel, G. R. Satchler, R. M. Drisko, and E. Rost, Phys. Rev. **128**, 2693 (1962).
[31] J. S. Blair, in *Lectures in Theoretical Physics*, edited by P. D. Kunz, D. A. Lind, and W. E. Brittin (University of Colorado Press, Boulder, Colo., 1966), p. 396.

range of the nuclear force and the finite size of the heavy incident particle. Baron *et al.*[32] used the value $R_{HP}=1.46A^{1/3}$ in the analysis of their data, and thus the β_L they report were corrected by the ratio 1.46/1.2. Bruge *et al.*[33] do not list the interaction radius used in their analysis, but give the $B(EL\uparrow)$ directly in SPU. The analysis of the deuteron scattering of Jolly[34] yielded a R_{HP} of 1.2, so no correction was necessary. Kim and Cohen[35] evaluate from a known $B(EL)$ the constant in

$$B(EL\uparrow)=\text{const}\times Z^2\times\beta^L,$$

and any R_{HP}/R_0 correction would be included in this constant.

The reduced transition probabilities obtained by the α-particle scattering are factors of 1.5–2.5 larger than our $B(EL\uparrow)$ values. The enhancement factors R_{HP}/R_0 were 1.4 for the $L=2$ and 1.7 for the $L=3$ case. The (d, d') results have quite large errors (40%), and are difficult to assess.

Coulomb Excitation

Coulomb excitation theory relates the $B(EL)$ directly to the observed excitation and should yield values of $B(EL)$ obtained that are quite accurate. The Oak Ridge[36] values of $B(E2)$ provide the best agreement with the values obtained in this experiment. The $B(E3)$'s of Alhazov[37] are larger than ours, and agree more with those of Baron *et al.*[32] and Bruge *et al.*[33]

Resonance Florescence

From the width Γ of the resonance scattering of γ rays from a given excited state, the $B(EL)$ to that excited state can be determined using the relation

$$B(EL)=\{L[(2L+1)!!]^2/8\pi(L+1)\}(c/\omega)^{2L+1}\Gamma.$$

The $B(E2)$'s quoted[38,39] in Table VI are in agreement with our result in one case, and are larger than our result in the other two cases.

V. SUMMARY AND CONCLUSION

Presented herein are the angular distributions of 60-MeV electrons inelastically scattered from the first quadrupole and octupole states of Sn^{116}, Sn^{118}, and Sn^{120}. It is shown that employing a distorted-wave calculation, a hydrodynamical model can be fitted to the data, yielding parameters of a transition charge density peaked somewhat within the nuclear surface. This transition charge yields values of the reduced transition probabilities which are consistent (in that they are enhanced) with the collective model assumed, and in qualitative agreement with values deduced from other experiments.

Does the surface-peaked transition charge satisfactorily account for the data? The answer is no, on two counts. First, if the present error analysis is correct, the χ^2 criteria of fit listed in Table V indicates that even the best fit is unsatisfactory. This may indicate that a transition charge of the form of Eq. (7) does not properly fit the data.

A second and more convincing argument is obtained by comparing the present $B(E2)$ values with the very accurate values recently published by Stelson *et al.*[40] From a very careful Coulomb excitation experiment they quote values of $B(E2, 0\rightarrow2)$ in e^2 F^4 of 2350 for Sn^{116}, 2480 for Sn^{118}, and 2300 for Sn^{120} with errors of $\pm5\%$ absolute and $\pm2\%$ relative. Comparing these values with Table V, we seen that the Coulomb excitation values are in rather good agreement with the Tassie model values, but disagree with the best-fit values. Yet Fig. 14 shows convincingly that the Tassie model does not fit the electron scattering data. Again, transition charges of the form of Eq. (7) fail to fit the experiments.

Although the Tassie model has given adequate fits notably for Ni (Ref. 9) and Pb (Ref. 12), the form of Eq. (7) is based on a crude nuclear model. Viewing Fig. 13 in detail, it appears that the theoretical curves are too high in the two points of the lowest momentum transfer, implying that Eq. (7) has too great an amplitude as its outer tail. It will be very interesting to see whether more sophisticated models can successfully account for the Coulomb excitations and the electron scattering data.

ACKNOWLEDGMENTS

Much of the initial development of the electron scattering apparatus was performed by Professor G. A. Peterson and Dr. M. A. Duguay. The analysis of our data was facilitated by the use of code DEULS, and by the explanations provided by Dr. L. E. Wright and S. Tuan of Duke University, Dr. D. Onley of Ohio University, and Dr. J. Ziegler, now at IBM. Within our own laboratory, the conscientious technical support provided by Edmond Comeau greatly aided our experiment. Professor Frank Firk was very helpful in setting up the on-line computation. L. S. Cardman and

[32] N. Baron, R. F. Leonard, J. L. Need, W. M. Stewart, and V. A. Madsen, Phys. Rev. **146**, 861 (1966); N. Baron, R. F. Leonard, J. L. Need, and W. M. Stewart, NASA Report No. TN-D-3067, 1965 (unpublished).

[33] G. Bruge, J. C. Faivre, H. Faraggi, T. Saudinos, and G. Vallois, Phys. Letters **13**, 244 (1964).

[34] R. K. Jolly, Phys. Rev. **139B**, 318 (1965).

[35] Y. S. Kim and B. L. Cohen, Phys. Rev. **142**, 788 (1966).

[36] P. H. Stelson and K. F. McGowan, Phys. Rev. **110**, 489 (1958); Nucl. Phys. **32**, 652 (1962).

[37] D. G. Alhazov, Y. P. Gangrskii, I. K. Lemberg, and Y. I. Undralov, Izv. Akad. Nauk. SSSR Ser. Fiz. **28**, 232 (1964).

[38] N. Lingappa, E. Kondaiah, C. Badrinathan, M. D. Deshpande, and M. Balakrishnan, Nucl. Phys. **38**, 146 (1962).

[39] B. Hrastnik, V. Knapp, and M. Vlatkovic, Nucl. Phys. **89**, 412 (1966).

[40] P. H. Stelson, F. K. McGowan, R. L. Robinson, W. T. Milner, and R. O. Sayer, Phys. Rev. **170**, 1172 (1968).

W. D. Metz assisted in data acquisition and reduction. Joseph Berti designed much of the apparatus, constructed in our shop by A. Comeau and J. Cimino, while Miss Kathy Lappert provided many excellent drawings. Dependable operations of the accelerator were provided by P. Jewett, W. Knudsen, S. Clow, R. Rondoe, M. Garfield, and F. Hegedus. Finally, our thanks go to Professor Howard Schultz, director of the Electron Accelerator Laboratory, for his continuing interest in the electron scattering project.

PHYSICAL REVIEW VOLUME 184, NUMBER 4 20 AUGUST 1969

Magnetic Moment of Sm^{145} and Attenuation Following the Decay of Oriented Sm^{145}*

MORTON KAPLAN,† J. BLOK,‡ AND D. A. SHIRLEY§

Department of Chemistry and Lawrence Radiation Laboratory, University of California, Berkeley, California 94720

(Received 15 November 1968)

Samarium-145 nuclei were oriented at low temperatures in neodymium ethylsulfate (NES) and cerium magnesium nitrate (CMN) lattices. From the temperature-dependent angular distribution of the 61-keV γ ray in Pm^{145}, a magnetic moment $\mu=0.92\pm0.06\,\mu_N$ was deduced for the ground state of Sm^{145}. The ratio of attenuation coefficients in the 61-keV state of Pm^{145} in the two lattices was found to be $G_2(\mathrm{CMN})/G_2(\mathrm{NES})=+0.44(10)$. Evidence is presented which indicates that temperature gradients in CMN can lead to erroneously low values for magnetic moments.

INTRODUCTION

RADIOACTIVE isotopes of most of the rare-earth elements have been oriented in lattices of neodymium ethylsulfate $Nd(C_2H_5SO_4)_3\cdot 9H_2O$ or of cerium magnesium nitrate $Ce_2Mg_3(NO_3)_{12}\cdot 24H_2O$.[1] In a systematic survey of oriented rare-earth nuclei in these lattices started in 1960, we obtained results for Sm^{145} that we could not explain. The magnetic moments derived from studies in the CMN and NES lattices were apparently quite different. While some of the earlier work in the field of nuclear orientation showed discrepancies of this kind, most of these could be attributed to poor experimental technique and would dispapear when the work was done more carefully. Our Sm^{145} results were checked for all the known sources of error, however, and refinement of technique only confirmed them. With the recent discovery that the temperature scales in use for both NES and CMN were seriously in error, the Sm^{145} data were corrected to the new scales,[2,3] and the magnetic moments derived from the two salts are now in excellent agreement. The determination of this magnetic moment is described here.

Having fitted the nuclear orientation data to derive moments, one also obtains, for each lattice, A_2, the coefficient of $P_2(\cos\theta)$ in the γ-ray angular distribution function. This A_2 may have the full value $B_2U_2F_2$ implied by angular momentum theory alone, or it may be attenuated by a factor G_2 which describes reorientation in an intermediate state. For this case (i.e., the 61-keV, $t_{1/2}=2.6$-nsec state[4] of Pm^{145}), we have found substantial attenuation in the CMN lattice, as described below.

EXPERIMENTAL

The Sm^{145} activity was prepared by neutron irradiation of enriched Sm^{144}, followed by ion-exchange separation from other rare-earth contaminants, notably (daughter) Pm^{145}, immediately before use. The Pm^{145}/Sm^{145} γ-ray intensity ratio was easily kept below 1%. Because the Pm^{145} γ rays were shown in separate experiments to be essentially isotropic, no correction was necessary.

The heavier rare earths grow substitutionally into the CMN lattice poorly, the difficulty increasing with Z.

* Work performed under the auspices of the U.S. Atomic Energy Commission.

† Permanent address: Department of Chemistry, Yale University, New Haven, Conn.

‡ Present address: General Electric Co., Schenectady, N.Y.

§ National Science Foundation Senior Postdoctoral Fellow 1966–7.

[1] D. A. Shirley, Ann. Rev. Nucl. Sci. **16**, 89 (1966).

[2] R. B. Frankel, D. A. Shirley, and N. J. Stone, Phys. Rev. **140**, A1020 (1965).

[3] J. Blok, D. A. Shirley, and N. J. Stone, Phys. Rev. **143**, 78 (1966).

[4] A. R. Brosi, B. H. Ketelle, H. C. Thomas, and R. J. Kerr, Phys. Rev. **113**, 239 (1959).